PHYSICAL REVIEW C **78**, 031303(R) (2008)

# Enhanced strength of the $2_1^+ \rightarrow 0_{g.s.}^+$ transition in $^{114}$Sn studied via Coulomb excitation in inverse kinematics

P. Doornenbal,[1,2,*] P. Reiter,[1] H. Grawe,[2] H. J. Wollersheim,[2] P. Bednarczyk,[2,3] L. Caceres,[2,4] J. Cederkäll,[5,6] A. Ekström,[6] J. Gerl,[2] M. Górska,[2] A. Jhingan,[7] I. Kojouharov,[2] R. Kumar,[7] W. Prokopowicz,[2] H. Schaffner,[2] and R. P. Singh[7]

[1]*Institut für Kernphysik, Universität zu Köln, D-50937 Köln, Germany*

[2]*Gesellschaft für Schwerionenforschung mbH, D-64291 Darmstadt, Germany*

[3]*The Niewodniczanski Institute of Nuclear Physics, Polish Academy of Sciences, 31-342 Krakow, Poland*

[4]*Departamento de Física Teórica, Universidad Autonoma de Madrid, E-28049 Madrid, Spain*

[5]*PH Department, CERN, 1211 Geneva, Switzerland*

[6]*Department of Physics, Lund University, 22100 Lund, Sweden*

[7]*Inter-Univerisity Accelerator Centre, New Delhi 110 067, India*

(Received 18 July 2008; published 22 September 2008)

The $2_1^+$ states of $^{114,116}$Sn were excited in two consecutive experiments by means of Coulomb excitation in inverse kinematics on a $^{58}$Ni target. A precise determination of the reduced transition probability $B(E2; 0_{g.s.}^+ \rightarrow 2_1^+)$ of $^{114}$Sn relative to the well-known $2_1^+$ excitation strength in $^{116}$Sn was achieved by comparing the relative projectile to target $2_1^+ \rightarrow 0_{g.s.}^+$ decay intensities. The obtained $B(E2\uparrow)$ value of 0.232(8) $e^2$b$^2$ for $^{114}$Sn confirms the tendency of large $B(E2\uparrow)$ values for the light tin isotopes below the midshell $^{116}$Sn that has been observed recently in various radioactive ion beam experiments. The result establishes most clearly the discrepancy between the current $B(E2\uparrow)$ value predictions from large-scale shell-model calculations and the experimental deviation, which commences already for the stable $^{114}$Sn isotope.

DOI: 10.1103/PhysRevC.78.031303 PACS number(s): 23.20.Js, 25.70.De, 27.60.+j

The ongoing development of new research facilities for experiments with unstable exotic nuclei has enabled nuclear structure investigations far away from the line of $\beta$ stability. Most especially, the structure around $^{100}$Sn has been spotlighted recently by experimental and theoretical research, as it is presumably the heaviest, particle bound, doubly magic $N = Z$ nucleus. In this context, the systematic study of nuclear properties along the semi magic, $Z = 50$ tin isotopes is of grand interest because the evolution of the proton gap can be experimentally probed in between two major shell closures.

The excitation energies from the ground state (g.s.) to the $2_1^+$ state between $^{102}$Sn and $^{130}$Sn are well established and possess an almost constant value [1], which is expected for semimagic nuclei in the generalized seniority scheme (see, e.g., Ref. [2]). A sensitive probe for the robustness of the $Z = 50$ shell closure along the chain of even tin isotopes between the two neutron shell closures at $N = 50$ and $N = 82$ is provided by the reduced transition probability, the $B(E2; 0_{g.s.}^+ \rightarrow 2_1^+)$ value, henceforth abbreviated as $B(E2\uparrow)$. The $E2$ transition strengths in stable even tin isotopes ($^{112-124}$Sn) are accurately known except for that of $^{114}$Sn. For this nucleus, the values obtained have been measured in two independent ways thus far with considerable errors that do not allow a firm conclusion on the evolution of the $B(E2\uparrow)$ value at this isotope. The small natural abundance of the $^{114}$Sn isotope of just 0.65% and the fact that $^{114}$Sn and $^{116}$Sn have almost identical $2_1^+$ level energies of 1299.907(7) and 1293.560(8) keV [1], respectively, impedes the direct approach via Coulomb excitation on a natural tin target. In two experiments with enriched $^{114}$Sn targets values of 0.20(7) $e^2$b$^2$ and 0.25(5) $e^2$b$^2$ were obtained [3,4]. More recently, Doppler-shift attenuation lifetime measurements were performed and values of 0.27(9) $e^2$b$^2$ and 0.19(4) $e^2$b$^2$ were deduced [5,6]. All these results lead to an accepted value of 0.24(5) $e^2$b$^2$ [1] with a considerable experimental uncertainty.

For unstable nuclei, lifetime measurements from, e.g., fusion-evaporation reactions are hindered by higher-lying isomeric states in the ns range. The $B(E2\uparrow)$ values are thus accessible preferentially via Coulomb excitation from the ground state employing radioactive beam techniques. On the neutron-rich side, this has been achieved recently [7]. For the proton-rich side, several Coulomb excitation experiments have been performed at relativistic, intermediate, and subbarrier energies for the nuclei $^{106,108,110}$Sn [8–11]. The derived $B(E2\uparrow)$ values from these experiments are plotted in Fig. 1 together with the excitation strengths of stable tin nuclei evaluated in Ref. [1]. Two different trends are observed for the chain of tin nuclei: while at the neutron-rich side drop considerably with increasing neutron number, an almost constant plateau of high $B(E2\uparrow)$ values emerges on the proton-rich side.

These unexpectedly high $B(E2\uparrow)$ values caused a persistent discrepancy between the results of new large-scale shell model (LSSM) calculations [8] and experimental findings. The LSSM calculation, using a polarization charge of 0.5 $e$ for protons and neutrons, has been performed with admixtures of up to $4p4h$ proton excitations across the $Z = 50$ shell gap to enhance the transition strength considerably over a pure neutron valence space calculation with a closed $Z = 50$ core [8,10]. In the latter approach the enhancement is achieved by introducing an effective neutron charge of 1.0$e$. Both calculations, however, yield a parabolically shaped systematics of the $B(E2\uparrow)$ with mass number $A$ and fail to reproduce the

*Present address: RIKEN Nishina Center for Accelerator-Based Science, Wako, Saitama 351-0198, Japan.

 

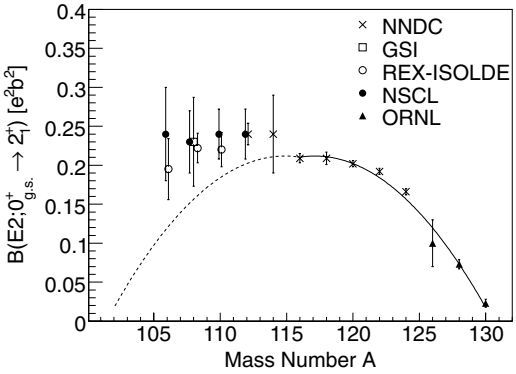


FIG. 1. Experimental $B(E2\uparrow)$ values in even-even tin isotopes. Data are taken from Refs. [1,7–11]. The statistical and systematic uncertainties of Ref. [9] were added quadratically. A parabolic fit has been applied to the nuclei ranging from $A = 116$–$130$ (solid line), which has been mirrored around $A = 116$ for the proton-rich side (dashed line).

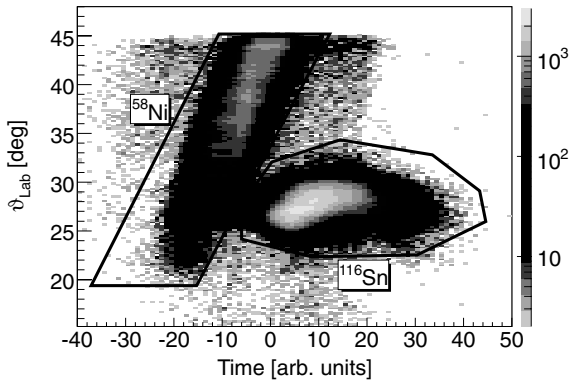


FIG. 2. Scattered projectile and target nuclei coincidences were detected in the PPAC for the $^{116}$Sn beam incident on the $^{58}$Ni target. The scattering angle is plotted versus the time of flight differences of both reaction partners. The corresponding kinematical cuts applied for coincident $\gamma$ rays are indicated. See text for details.

asymmetric trend of the experimental results. This is clearly demonstrated by the symmetric lower shell continuation (dashed line) of the parabola fitted to the $A = 116$–$130$ values (full line) to guide the eye.

The inaccurate $B(E2\uparrow)$ value of $^{114}$Sn motivated a Coulomb excitation experiment with a stable beam in inverse kinematics to improve this crucial data point and to firmly establish the location along the Sn isotope chain where the $B(E2\uparrow)$ value is increased. Because a stable tin beam does not suffer from low beam intensities, the $E2$ excitation strength can determined with a high accuracy from a $\gamma$-ray measurement. Two stable tin nuclei seem to belong to the region of enhanced $B(E2\uparrow)$ values: $^{112}$Sn and $^{114}$Sn. For the former nucleus previous Coulomb excitation results [3,4,12,13] have been confirmed recently by means of lifetime measurements employing the Doppler-shift attenuation method [14]. For $^{114}$Sn, the large experimental error prohibits definite conclusions about the exact $B(E2\uparrow)$ evolution. Therefore, we performed two consecutive Coulomb excitation experiments using $^{114}$Sn and $^{116}$Sn beams with "safe" beam energies well below the Coulomb barrier to determine the relative excitation strengths between both tin isotopes in inverse kinematics on the same target. In this way systematic errors can be excluded and the target excitation cancels for the $^{114}$Sn / $^{116}$Sn $\gamma$-ray yield ratio. These $\gamma$-ray yield data are a direct measure of the $B(E2\uparrow)$ ratio of $^{114}$Sn relative to $^{116}$Sn. Note that the adopted $B(E2\uparrow)$ value for $^{116}$Sn of $0.209(6)\,e^2b^2$ is an evaluation of fifteen different experimental results [1] and is, therefore, a reliable and precise reference point.

The tin beams were provided by the UNILAC accelerator at Gesellschaft für Schwerionenforschung (GSI) with an energy of $3.4A$ MeV. Beam particles were incident on a 0.7-mg/cm$^2$ $^{58}$Ni target with a purity of 99.9%. An annular gas-filled parallel plate avalanche counter (PPAC) was placed 13 cm downstream of the target to detect both the scattered projectiles as well as the recoiling target nuclei. The PPAC consisted of an anode foil, subdivided into 20 radial segments for the azimuthal angle $\varphi_{\rm lab}$ information, and a cathode plate of 50 concentrical rings connected by an electronic delay line with 2-ns time delay steps. The polar angle $\vartheta_{\rm lab}$ was deduced by measuring the delay line time differences between signals coming from the innermost and outermost ring. The PPAC covered an angular range of $15^\circ \leqslant \vartheta_{\rm lab} \leqslant 45^\circ$. Because the PPAC was split into two independent parts, kinematical coincidences between projectiles and ejectiles were measured within this angular range. For ejectiles detected in the PPAC, the corresponding scattering angles of $^{114}$Sn and $^{116}$Sn varied between $24^\circ \leqslant \vartheta_{\rm lab} \leqslant 31^\circ$. To identify projectile and target nucleus, the time of flight differences between both scattered particles was measured. Figure 2 shows the measured scattering angle of one detector half as a function of the time difference. The figure presents data from the $^{116}$Sn beam striking on the $^{58}$Ni target as an example. It demonstrates the unambiguous assignments of the measured scattering angles in both PPAC halves to projectile and target nucleus, respectively.

De-excitation $\gamma$ rays emitted after Coulomb excitation were measured with two Superclover (Ge) detectors mounted at an angle of $\vartheta_\gamma = 25^\circ$ relative to the beam axis in the forward direction at a distance of 20 cm from the target. Each detector consisted of four coaxial N-type Ge crystals, arranged like a four leaf clover. The two detectors had a total photopeak efficiency of $\approx$1% and an energy resolution of 3.8 keV [full width at half maximum (FWHM)] at 1332.5 keV. To suppress low energetic radiation, the front sides of the Superclover detectors were covered by a stacked shielding of 0.2-mm Ta, 1.0-mm Sn, and 0.5-mm Cu plates. Scattered particles hitting the PPAC had velocities of up to $\beta \approx 10\%$ for the target nuclei, whereas the projectiles retained velocities of up to $\beta \approx 6\%$. A Doppler correction was applied only when both reaction particles and at least one $\gamma$ ray were detected. Although the lower angular coverage of the PPAC was $\vartheta_{\rm lab} = 15^\circ$, two-particle events were detected only for target nucleus angles above $\vartheta_{\rm lab} \approx 20^\circ$. This restriction was caused by the low projectile residual energy for a high center-of-mass $\vartheta_{\rm c.m.}$ scattering angle and pertained to $^{114}$Sn and $^{116}$Sn in equal measure. Due to the PPAC polar angle resolution of $2^\circ$, the scattering angle of the projectile and, accordingly, the velocity were best determined by a reconstruction from the position information

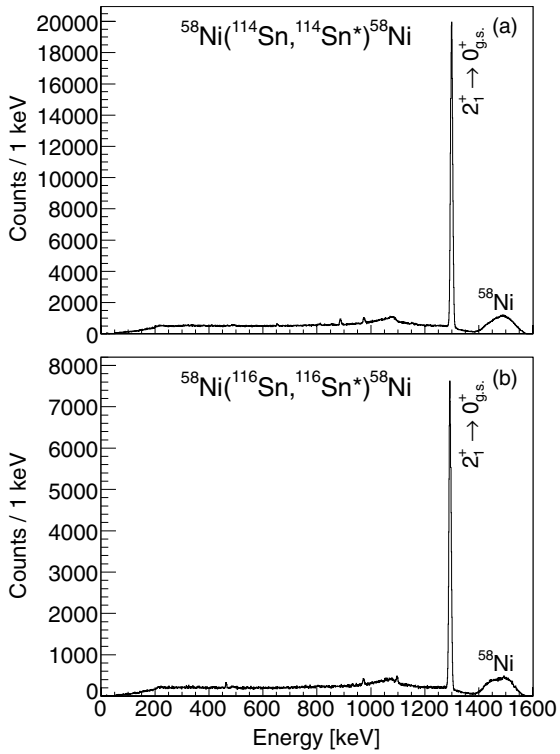


FIG. 3. Doppler corrected $\gamma$-ray spectra associated with a coincidence of two particles in the PPAC. The Doppler correction was applied using the kinematical information of the target nuclei but assuming a projectile excitation of $^{114}$Sn (a) and $^{116}$Sn (b), respectively. The elevation between 1400 and 1600 keV corresponds to decays from the $2^+_1$ state of the $^{58}$Ni ejectiles.

of the target nucleus and hence used for the Doppler correction. A $\gamma$-ray energy resolution of 0.7% (FWHM) was obtained for decays from projectile excitation and 1.0% (FWHM) for decays from target excitation. The difference was caused by the Doppler broadening due to the higher velocity of the latter particles. Figure 3 shows the Doppler-corrected spectra for projectile excitation of $^{114}$Sn and $^{116}$Sn. Clearly, the spectra are dominated by the the $2^+_1 \rightarrow 0^+_{\text{g.s.}}$ transitions. Higher excited states were only weakly populated. Namely transitions from the $0^+_2, 3^-_1, 4^+_1$ states to the respective $2^+_1$ state were detected with much lower intensity. In both cases the summed intensity from decays of higher-lying states added up to less than 4% of the $2^+_1 \rightarrow 0^+_{\text{g.s.}}$ decay intensity.

To obtain the $B(E2\uparrow)$ value in $^{114}$Sn, the experimental $\gamma$-ray intensity double ratio $I_\gamma(^{114}\text{Sn})/I_\gamma(^{58}\text{Ni})/I_\gamma(^{116}\text{Sn})/I_\gamma(^{58}\text{Ni})$ of the $2^+_1 \rightarrow 0^+_{\text{g.s.}}$ decays was determined. The observed feeding was subtracted from the $2^+_1$ intensities. The experimental double ratio was compared with Coulomb excitation calculations from the Winther-de Boer COULEX code [15]. The calculations included the feeding contributions from the $0^+_2, 3^-_1, 4^+_1$ states in $^{114}$Sn and $^{116}$Sn, which were obtained from the known excitation strengths given in Ref. [1]. The $0^+_{\text{g.s.}} \rightarrow 2^+_1$ matrix element in $^{114}$Sn was adjusted in the COULEX calculations to reproduce the experimental double ratio. As a result, the $B(E2\uparrow)$ value in $^{114}$Sn was determined as 0.232(8) $e^2$b$^2$. The error is the quadratic sum of the individual uncertainties of the $\gamma$-ray intensities (1%), the adopted $^{116}$Sn $B(E2\uparrow)$ value (3%), and the angular range acceptance of the PPAC (1%). The latter error accounted for slightly different particle detection efficiencies in $^{114}$Sn and $^{116}$Sn at high center-of-mass scattering angles and, accordingly, low projectile energies; and for different beam spots on the target in the two experiments ($\approx$3-mm deviation). It is noteworthy that the double ratio has a negligible dependence ($\ll$1%) on the selected scattering angle range if both ranges are identical and the singles ratios $I_\gamma(^{114,116}\text{Sn})/I_\gamma(^{58}\text{Ni})$ vary only slightly by less than 10% from the lowest accepted scattering angle ($\vartheta_{\text{c.m.}} = 90^\circ$) to the highest ($\vartheta_{\text{c.m.}} = 140^\circ$), respectively. In summary, the new $B(E2\uparrow)$ value of 0.232(8) $e^2$b$^2$ for the first excited $2^+$ state in $^{114}$Sn is a significant improvement with respect to the previous insufficient situation. Moreover, the new result is also, with its reduced error limits, clearly consistent with all previous values.

Our deduced $B(E2\uparrow)$ value of $^{114}$Sn is included in the experimental $B(E2\uparrow)$ systematics of Fig. 4 and shows, with the smallest uncertainty, an increased $B(E2\uparrow)$ value with respect to the neighboring midshell nuclei. Thus, our result demonstrates that the experimental asymmetry toward an enhanced $E2$ transition strengths commences with $^{114}$Sn as the anchor point for the deviating trend.

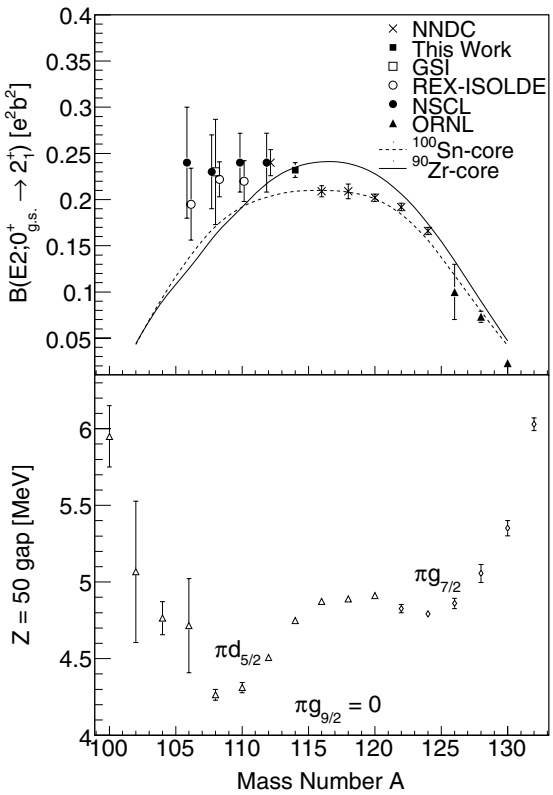


FIG. 4. The upper panel displays a comparison of the new experimental $B(E2\uparrow)$ value from the present work and data from Refs. [1,7,8,10,11] for even-even tin isotopes with LSSM calculations presented in Ref. [8] using a $^{100}$Sn (dotted line) and $^{90}$Zr (solid line) closed-shell core, respectively. The lower panel shows the experimental $Z = 50$ gaps extracted from Refs. [18,19].

Within the work on $^{108}$Sn by Banu and collaborators [8], the $B(E2\uparrow)$ values for the $Z = 50$ tin isotopes have been determined theoretically by means of state-of-the-art large-scale shell-model calculations. These calculations used an effective interaction derived with the $G$-matrix prescription [16] from the CD-Bonn nucleon-nucleon potential [17] with the two different closed shell cores of $^{90}$Zr ($SM_{\pi\nu}$) and $^{100}$Sn ($SM_{\nu}$), respectively. $SM_{\pi\nu}$ uses a proton $\pi(g, d, s)$ and neutron $\nu(g_{7/2}, d_{5/2}, s_{1/2}, h_{11/2})$ model space. Up to $4p4h$ excitations were allowed across the $Z = 50$ closed shell and $B(E2\uparrow)$ values were calculated with a common polarization charge of $0.5\,e$ for protons and neutrons. For $SM_{\nu}$ a pure neutron $\nu(g_{7/2}, d_{5/2}, s_{1/2}, h_{11/2})$ model space and an effective neutron charge of $1.0\,e$ were employed to account for the neglect of proton core excitations. For both cases, the theoretical curve is parabolic and symmetric with respect to the midshell nucleus $^{116}$Sn, as shown in Fig. 4, causing the puzzling discrepancies between experiment and theory for the lighter tin isotopes. The $SM_{\pi\nu}$ calculation agrees with the new experimental $^{114}$Sn $B(E2\uparrow)$ of the present work, but overpredicts the $A \geqslant 116$ values, whereas the lower-shell values seem to be underestimated despite of the large experimental uncertainties. Similarly, the $SM_{\nu}$ approach agrees with the upper-shell values but underpredicts the $E2$ strengths in the light Sn isotopes.

Since the LSSM calculations presented with the first radioactive beam experiment on $^{108}$Sn [8], recent experiments on $^{106-110}$Sn [9–11] confirmed the deviation from a symmetric behavior of the $B(E2\uparrow)$. Several qualitative arguments for future improvements of shell-model calculations, such as excitations across the $N = 50$ shell [8], $\alpha$ correlations due to proton $2p2h$ excitations [9], refined tuning of proton-neutron monopoles [8,10], or even a reduction of the $Z = N = 50$ shell gaps [11] have been brought forward. In the lower panel of Fig. 4 the experimental $Z = 50$ shell gaps are shown for $N = 50$–$82$ [18]. The $^{100}$Sn value was extrapolated from experimental proton $g_{9/2}$ and $d_{5/2}$ single-particle energies in $^{90}$Zr by using empirical two-body matrix elements including Coulomb repulsion [19]. From $^{132}$Sn, the well-known reduction of the proton gap toward the neutron midshell is observed, which is due to proton-neutron induced cross-shell excitations. The gap stays constant between $N = 76$ and 66 with the $\pi g_{7/2}$ and $\pi d_{5/2}$ crossing at $N = 70$. Below $N = 66$ ($A = 116$) the gap reduces gradually by about 600 keV before it increases toward the double shell closure at $N = 50$. This is exactly the region where the $B(E2\uparrow)$ values deviate from symmetry and the shell-model trend. It is known from LSSM calculations [8] that the major contribution to the $B(E2\uparrow)$ stems from proton excitations across $Z = 50$, as can be inferred from the $t = 0$ and $t = 4$ curves in Fig. 3 of Ref. [8]. Moreover, these excitations are dominated by the large stretched $\pi g_{9/2} \rightarrow \pi d_{5/2}$ $E2$ matrix element. In terms of monopole driven shell evolution [20–23], the reduction of the shell gap can be clearly attributed to the emptying of the neutron $\nu g_{7/2}$ orbit below $N = 66$. This will lift the $\pi g_{9/2}$ relative to the $\pi d_{5/2}$ and hence reduce the gap, which is decisive for $E2$ core polarization. The respective monopoles $V^m(\pi g_{9/2}\nu j)$ are largely different for the $g_{9/2}$ spin flip partner $j = g_{7/2}$ and $j = d_{5/2}$ [20,22–24]. This causes the experimentally well-established dramatic decrease of the $\nu g_{7/2}$-$\nu d_{5/2}$ distance in $N = 51$ isotones on filling of the $\pi g_{9/2}$ orbit between $^{91}$Zr and $^{101}$Sn (see, e.g., Ref. [24]) and acts in a similar way on the $\pi g_{9/2}$ orbit when filling (respective emptying) the $\nu g_{7/2}$ shell along the $Z = 50$ isotopic chain. The decrease is less pronounced due to the near degeneracy of the neutron $g_{7/2}$ and $d_{5/2}$ orbits leading to a simultaneous filling (emptying) of the two and to the effect of the smaller $\nu g_{7/2}$-$\pi d_{5/2}$ monopole $V^m(\pi d_{5/2}\nu g_{7/2})$. It is therefore concluded that (i) proton excitations across a reduced $Z = 50$ gap are responsible for the enhanced $B(E2\uparrow)$ values below $A = 116$ and that (ii) interactions used in LSSM calculations need monopole tuning to reproduce both the evolution of the experimental $Z = 50$ gap and the $B(E2\uparrow)$. It should be noted that the described scenario implies that in $^{102,104}$Sn the $B(E2\uparrow)$ values will return to be normal. For $^{100}$Sn, the empirical shell gap extrapolation results in a reduction of the proton gap of about 800 keV relative to the neutron gap [19].

In summary, we have determined the $B(E2\uparrow)$ value in $^{114}$Sn relative to the well-known value of $^{116}$Sn with a high accuracy. The deduced excitation strength of $0.232(8)\,e^2b^2$ marks the key starting point for the striking deviation from a symmetric trend around the $N = 66$ neutron midshell that was observed from radioactive beam experiments in the proton-rich $^{106-110}$Sn. This implies a disagreement with current large-scale shell-model calculations and suggests the need for a refined tuning of the two-body interactions employed. Further experimental studies as well as theoretical investigations of the $Z = 50$ and $N = 50$ gaps are of substantial importance to enlighten the nuclear structure in the vicinity of the doubly magic $^{100}$Sn.

The authors thank the GSI accelerator staff for providing the tin beams and appreciate shell-model discussions with F. Nowacki. One author (P.D.) is grateful for the support by the JSPS.

[1] S. Raman, C. W. Nestor, and P. Tikkanen, At. Data Nucl. Data Tables **78**, 1 (2001).
[2] R. Casten, *Nuclear Structure from a Simple Perspective* (Oxford University Press, New York, 2000).
[3] D. G. Alkhazov, D. S. Andreev, K. I. Erokhina, and I. K. Lemberg, Zh. Eksp. Teor. Fiz. **33**, 1347 (1957) [Sov. Phys. JETP **6**, 1036 (1958)].
[4] D. S. Andreev, V. D. Vasilev, G. M. Gusinskii, K. I. Erokhina, and I. K. Lemberg, Izv. Akad. Nauk SSSR, Ser. Fiz. **25**, 832 (1961); Columbia Tech. Transl. **25**, 842 (1962).
[5] I. N. Vishnevsky, M. F. Kudoyarov, E. V. Kuzmin, Yu. N. Lobach, A. A. Pasternak, and V. V. Trishin, in *Proceedings of the 41st Conference on Nuclear Spectroscopy and the Structure of the Atomic Nucleus, Minsk* (1991), p. 71.
[6] J. Gableske *et al.*, Nucl. Phys. **A691**, 551 (2001).
[7] D. C. Radford *et al.*, Nucl. Phys. **A752**, 264c (2005).
[8] A. Banu *et al.*, Phys. Rev. C **72**, 061305(R) (2005).
[9] C. Vaman *et al.*, Phys. Rev. Lett. **99**, 162501 (2007).
[10] J. Cederkäll *et al.*, Phys. Rev. Lett. **98**, 172501 (2007).

[11] A. Ekström *et al*., Phys. Rev. Lett. **101**, 012502 (2008).
[12] P. H. Stelson, F. K. McGowan, R. L. Robinson, and W. T. Milner, Phys. Rev. C **2**, 2015 (1970).
[13] R. Graetzer, S. M. Cohick, and J. X. Saladin, Phys. Rev. C **12**, 1462 (1975).
[14] J. N. Orce, S. N. Choudry, B. Crider, E. Elhami, S. Mukhopadhyay, M. Scheck, M. T. McEllistrem, and S. W. Yates, Phys. Rev. C **76**, 021302(R) (2007); Phys. Rev. C **77** 029902(E) (2008).
[15] A. Winther and J. De Boer, in *Coulomb Excitation*, edited by K. Alder and A. Winther (Academic Press, New York/London, 1966).
[16] M. Hjorth-Jensen, T. T. S. Kuo, and E. Osnes, Phys. Rep. **261**, 125 (1995).
[17] R. Machleidt, F. Sammarruca, and Y. Song, Phys. Rev. C **53**, R1483 (1996).
[18] A. H. Wapstra, G. Audi, and C. Thibault, Nucl. Phys. **A729**, 337 (2003).
[19] H. Grawe, K. Langanke, and G. Martínez-Pinedo, Rep. Prog. Phys. **70**, 1525 (2007).
[20] T. Otsuka, R. Fujimoto, Y. Utsuno, B. A. Brown, M. Honma, and T. Mizusaki, Phys. Rev. Lett. **87**, 082502 (2001).
[21] H. Grawe, Acta Phys. Pol. B **34**, 2267 (2003).
[22] H. Grawe, *Lecture Notes in Physics* (Springer, Berlin/ Heidelberg, 2004), Vol. 651, p. 33.
[23] T. Otsuka, T. Suzuki, R. Fujimoto, H. Grawe, and Y. Akaishi, Phys. Rev. Lett. **95**, 232502 (2005).
[24] H. Grawe, A. Blazhev, M. Gorska, R. Grzywacz, H. Mach, and I. Mukha, Eur. Phys. J. A **27**, s01, 257 (2006).